Journal of Ceramic Processing Research. Vol. 24, No. 2, pp. 321~328 (2023)
(Received 20 Septembert 2022, Received in revised form 18 October 2022, Accepted 8 December 2022)
https://doi.org/10.36410/jcpr.2023.24.2.321

JOURNAL OF
Ceramic Processing Research

Effects of different carbon sources on the phase composition and microstructure of synthesized SiC-B_4C composite powders

Yu Cao, Ruyi Deng, Jilin Hu*, Jinxiu He, Dapeng Lei, Zhanjun Chen* and Yangxi Peng
Modern Industry School of Advanced Ceramics, Hunan Provincial Key Laboratory of Fine Ceramics and Powder Materials, School of Materials and Environmental Engineering, Hunan University of Humanities, Science and Technology, Loudi, 417000, China

SiC-B_4C composite powders were synthesized by the carbothermal reduction method under an argon atmosphere using different kinds of carbon sources (carbon black and starch) and silica sol and boric acid as the precursor raw materials. Based on thermodynamic analysis and calculation, the effects of different carbon sources and reaction temperatures on the mass loss rate, phase composition, and microstructure of SiC-B_4C ultrafine composite powders were comparatively studied. Results showed that the optimum conditions for synthesizing SiC-B_4C composite powders with carbon black as the carbon source were 1550 ºC for 2 h, whereas the optimum conditions for synthesizing SiC-B_4C composite powders with starch as the carbon source were 1450 ºC-1550 ºC for 2 h. The powder samples synthesized with carbon black as the carbon source at 1550 ºC were mainly composed of flaky, columnar-like, spherical, and irregular polyhedral particles (about 100-200 nm in diameter). Mutual cohesion or agglomeration between particles was minimal. In the powder samples synthesized at 1550 ºC with an excess of 10 wt% starch, in addition to a certain amount of flaky, spherical, and other irregular structure particles, a certain amount of uniform, slender whiskers (about 50-100 nm in diameter) and a certain phenomenon of lap and winding between the whiskers were noted. The powder samples synthesized at 1550 ºC with an excess of 20 wt% starch had no whisker-like substance.

Keywords: carbon black, starch, SiC-B_4C, composite powders, synthesis.

Introduction

As an important advanced ceramic material, SiC ceramic has excellent comprehensive properties such as high-temperature strength, high hardness, and strong chemical corrosion resistance, and becomes the focus of current domestic and foreign research [1-4]. However, due to the poor fracture toughness (<3.5 MPa $m^{1/2}$) and low-room-temperature strength of SiC ceramics, its application range is limited [5-7]. Boron carbide (B_4C) has a series of excellent properties, such as high hardness, low density, high-temperature resistance, good chemical stability, and high fracture toughness. These characteristics make it widely used in the grinding of hard materials, lightweight bullet-resisting armor, advanced refractory materials, and rocket solid fuels in various fields [8, 9]. Many related reports have combined B_4C with SiC to prepare SiC-B_4C composites to realize the complementary advantages of these two materials in performance [10-14].

To prepare high-performance SiC-B_4C composites, preparing high-quality SiC-B_4C composite powders with high purity and fine particles is very important. Generally, the preparation methods of carbide ultrafine powders mainly include carbothermal reduction, self-propagating high-temperature synthesis, sol-gel synthesis, and chemical vapor deposition. Song et al. [15] prepared titanium carbide powders with octahedral and columnar structures by the carbothermal reduction method combined with the molten salt method. Wang et al. [16] successfully synthesized nanoscale wolframium carbide powders with high BET values based on a low-temperature carbothermal reduction. Najafi et al. [17] synthesized SiC-B_4C nano powders in a water-solvent-catalyst-dispersant system by the sol-gel synthesis method. The particle size of the synthesized SiC-B_4C powders was between 20-40 nm with a surface area of 172.92 m^2/g and a uniform morphology. Tu et al. [18] prepared amorphous-nanocrystalline B_4C films with a thickness of 0.2-1.9 μm by chemical vapor deposition.

Carbothermal reduction is the most important method for preparing carbide ceramic powders in modern industry. At present, reports on the synthesis of SiC-B_4C composite powders by carbothermal reduction are few. Liu et al. [19] successfully prepared SiC-B_4C composite powders with a uniform B_4C distribution by pre-adding SiC using boric acid (H_3BO_3), graphite, and petroleum coke as the raw materials. Parlakyigit et al. [20] directly synthesized SiC-B_4C composite powders by the carbothermal reduction method by adding Si

---

*Corresponding author:
Tel : +86 738 8325065
Fax: +86 738 8325304
E-mail: hujilin@126.com (J. Hu), chen829924@163.com (Z. Chen)

powder to the precursor solution made of H_3BO_3 and sucrose base.

To improve the properties of SiC-B_4C composite powders further, the present work synthesizes SiC-B_4C composite powders by the carbothermal reduction method at high temperatures in an argon atmosphere using different types of carbon sources (carbon black and starch) and silica sol and H_3BO_3 as the raw materials. Based on thermodynamic analysis and calculation, the effects of different carbon sources and reaction temperatures on the mass loss rate, phase composition, and microstructure of the synthesized SiC-B_4C composite powders are comparatively studied.

Experimental

Silica sol (SiO_2, 28 wt%, Hunan Changsha Water Glass Factory, China), H_3BO_3 (≥99.0% purity, Sinopharm Chemical Reagent Co., Ltd, China), and carbon black (C, ≥99.0% purity, Fujian Nanping Rongxin Chemical Co., Ltd, China) were used as the starting materials for the preparation of SiC-B_4C composite powders. The preparation of the SiC-B_4C composite powders is shown in Fig. 1. The amounts of silica sol, H_3BO_3, and carbon black were adjusted to yield a SiC/B_4C molar ratio of 6:4. All the starting materials were accurately weighed according to reactions (1) and (2). These ingredients were uniformly mixed in a magnetic stirrer for 2 h using ethanol as the liquid medium. The well-mixed precursor slurry was dried in a vacuum blast-drying oven at 110 °C for 24 h, ground in a mortar, and then placed in a ceramic ark. In a high-temperature tubular electric furnace, heating was performed at a rate of 10 °C min^{-1} in an argon atmosphere, and high-temperature synthesis reaction was carried out at 1350 °C, 1450 °C, and 1550 °C for 2 h. After the holding time, when the temperature in the furnace was cooled naturally to room temperature, the synthesized powders were obtained. The carbon black raw material in the above formula was replaced with starch (≥99.0% purity), and the above experimental process was repeated to synthesize the SiC-B_4C composite powders. During the high-temperature synthesis reaction, in addition to the decomposition of organic starch to produce elemental carbon and gaseous water, gaseous substances such as C_xH_y and CO_x were generated, which led to the loss of carbon content in the system. Therefore, the starch dosage in the formula was designed to be in excess of 10 wt% and 20 wt%. The masses of the powder samples before and after reaction were measured by an electronic analytical balance to determine the extent of the synthesis reaction. According to the mass of the powder samples before and after the synthesis reaction, the weight loss rate of the samples was calculated. The phase composition of the synthesized powder samples was analyzed by an X-ray diffractometer (XRD, Y2000). The microstructure of the powder samples was observed by using a scanning electron microscope (SEM, Zeiss Sigma 500).

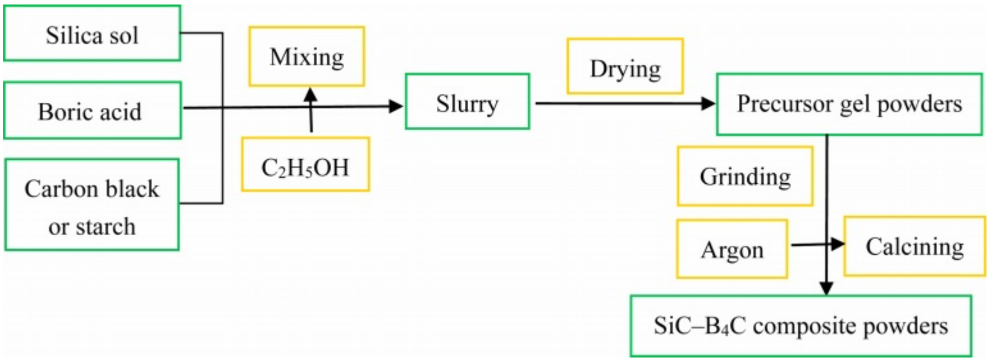

Fig. 1. Preparation of SiC-B_4C composite powders.

Results and Discussion

Thermodynamic analysis

In this paper, only thermodynamic calculations were performed for the reaction system using carbon black as the carbon source because starch decomposes to form elemental carbon at low temperatures. The synthesis reactions of H_3BO_3, silica sol, and carbon black at high temperatures are as follows [5, 21]:

$$SiO_2\ (s) + 3C\ (s) = SiC(s) + 2CO\ (g) \tag{1}$$

$$7C + 4H_3BO_3 = B_4C + 6CO + 6H_2O \tag{2}$$

From $\Delta G^\theta = \Delta H^\theta - T\Delta S^\theta$, Equation (3) can be obtained:

$$\Delta G = \Delta H^\theta - T\Delta S^\theta + RTln\ (P_{CO}/P^\theta) \tag{3}$$

Among them, ΔG^θ is the standard Gibbs free energy of the substance; R is the gas constant; T is the thermodynamic temperature; P^θ and P_{CO} are the standard atmospheric pressure and the partial pressure of CO, respectively.

Substituting the thermodynamic data of each substance in Equations (1) and (2) into (3), the expression of ΔG in Equations (4) and (5) can be obtained:

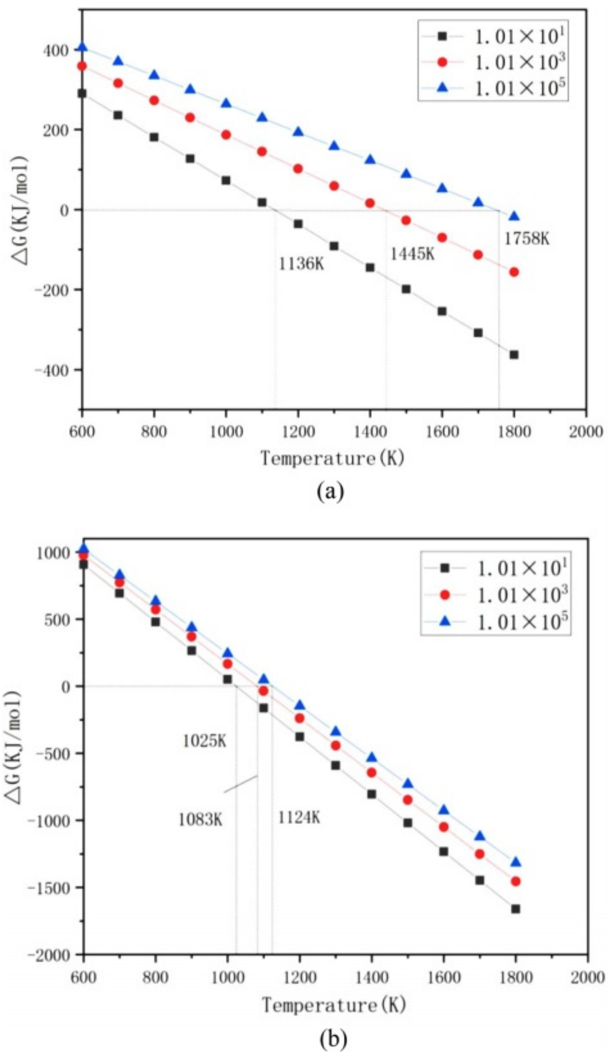

Fig. 2. Variation of Gibbs free energy (ΔG) with temperature (T) under different CO partial pressures for (a) reaction (1) and (b) reaction (2).

$$\Delta G_1 = 616680 – 352.67T + 2\times 8.3145\times T\ln (P_{CO}/P^{\theta}) \quad (4)$$

$$\Delta G_2 = 2192150 – 1949.31T + 2\times 8.3145\times T\ln (P_{CO}/P^{\theta}) \quad (5)$$

Taking the values of P_{CO} as 1.01×10^1 Pa, 1.01×10^3 Pa, and 1.01×10^5 Pa, and the value of P^{θ} as 1.01×10^5 Pa, and substituting the above values into Equations (4) and (5), the variation of the calculated Gibbs free energy (ΔG) with temperature (T) is shown in Fig. 2.

Fig. 2 shows that taking standard atmospheric pressure as an example, from a thermodynamic point of view, when the ΔG of Equations (1) and (2) is 0, the corresponding temperatures are 1445 K and 1083 K, respectively. Theoretically, if the actual synthesis temperature is higher than these two temperatures, SiC and B$_4$C can be generated. Under vacuum conditions, when the ΔG of Equations (1) and (2) is 0, the corresponding reaction temperature decreases. When the P_{CO} is 1.01×10^1 Pa, 1.01×10^3 Pa, and 1.01×10^5 Pa, and the reaction temperatures in Equations (1) and (2) are 1136 K and 1025 K, 1445 K and 1083 K, 1758 K and 1124 K, respectively, the two ΔG is 0, indicating that the two ΔG decreases remarkably with increasing temperature and decreasing P_{CO}. Therefore, under the condition of high temperature and low pressure, the synthesis reaction of SiC and B$_4$C is more favorable [5, 22].

Mass loss rate analysis

When carbon black or starch is selected as the carbon source, gaseous substances such as CO are generated during the synthesis of SiC-B$_4$C composite powders under high-temperature reaction conditions. Gaseous substances such as H_2O are generated with starch as carbon source at high temperatures. Moreover, the gaseous substances generated escape, resulting in the reduction of the quality of the powder samples after calcination. Therefore, the mass loss rate can be calculated according to the mass difference of the powder samples before and after calcination, and the degree of the reaction for synthesizing SiC-B$_4$C composite powders under different conditions can be inferred. In this paper, the ratio of the measured weight loss rate to the theoretical weight loss rate (relative weight loss rate) is used to judge the degree of the synthesis reaction. The change of relative weight loss rate with reaction temperature during the synthesis of SiC-B$_4$C composite powders is shown in Table 1.

Table 1 shows that whether the carbon source selected is carbon black or starch, the relative weight loss rate of the powder samples increases with the increase of the reaction temperature. When the reaction temperature is 1350 °C, the relative weight loss rate is only 26.2% with carbon black as the carbon source, and when the reaction temperature increases to 1550 °C, the relative weight loss rate reaches 106.8%, which is 6.8% higher than the theoretical mass loss rate (100.0%) of the powder samples. The main reasons why the actual mass loss rate at 1550 °C exceeds the theoretical mass loss rate are as follows: On the one hand, a small part of the intermediate SiO generated in the system during the synthesis may escape from the system together with the CO flowing argon [23]. On the other hand, it may be caused by gaseous B_2O_3 produced by the thermal decomposition of H_3BO_3 in the raw material at high temperatures escaping with a small amount of other gases [24].

When starch is selected as the carbon source, with the increase in the reaction temperature, the weight loss rate is generally higher than that of the powder samples with carbon black as the carbon source because in the actual synthesis reaction, organic starch not only decomposes into elemental carbon and water gaseous substances but also generates gaseous substances such as CO, CO_2, and C_xH_y, resulting in a higher mass loss rate of the powder samples [25]. When the reaction

Table 1. Relationship between relative mass loss rate and reaction temperature for powder samples.

Carbon source	Holding time (h)	Reaction Temperature (ºC)	Relative mass loss rate (%)
carbon black	2	1350	26.2
carbon black	2	1450	88.6
carbon black	2	1550	106.8
10 wt% excess of starch	2	1350	30.9
10 wt% excess of starch	2	1450	86.3
10 wt% excess of starch	2	1550	110.9
20 wt% excess of starch	2	1350	42.5
20 wt% excess of starch	2	1450	101.3
20 wt% excess of starch	2	1550	113.9

temperature is 1450 °C, the relative weight loss rates of powder samples with 10% and 20% excess starch as the carbon source are 86.3% and 101.3%, respectively; when the reaction temperature increases to 1550 °C, the weight loss rate reaches 110.9% and 113.9%, respectively. The actual mass loss rate of powder samples in the synthesis reaction exceeds the theoretical mass loss rate mainly due to the escape of SiO, H_3BO_3, and gaseous substances (such as CO, CO_2, C_xH_y generated by starch decomposition).

Phase composition analysis

Fig. 3 shows the XRD patterns of the precursor mixed powder and the powder samples prepared after being kept for 2 h at different reaction temperatures with carbon black as the carbon source. Reaction temperature has a great influence on the phase composition of the synthesized powder samples. Mainly characteristic diffraction peaks of B_2O_3 are in the precursor mixed powder [26]. No evident characteristic diffraction peaks of carbon black are found in Fig. 3(a), indicating that the carbon black raw material mainly exists in an amorphous form. In addition, no SiO_2 diffraction peak is observed, indicating that the SiO_2 component in the silica sol raw material exists in the mixture in an amorphous manner, which is consistent with the research results of the literature [27] (the characteristic diffraction peaks of SiO_2 are not found in the system after incubation at 1400 °C for 2 h). Only the characteristic diffraction peaks of B_2O_3 still exist in the powder samples synthesized at 1350 °C for 2 h, but the intensity of the diffraction peaks of B_2O_3 decreases, indicating that a small amount of B_4C is synthesized at this reaction temperature (it is not shown in the XRD pattern due to the relatively small amount generated). When the reaction temperature reaches 1450 °C, weak characteristic diffraction peaks of SiC and B_4C are in the XRD pattern of the synthesized powder samples, the diffraction peak of B_2O_3 completely disappears, and no other diffraction peaks are found, indicating that a small amount of B_4C and SiC is formed in the system at this reaction temperature. When the reaction temperature continues to rise to 1550 °C, the diffraction peaks of SiC and B_4C in the XRD pattern become the two most important kinds of characteristic diffraction peaks, and become sharper, indicating that the carbothermal reduction reaction is complete at this reaction temperature. Combined with the mass loss rate (see Table 1), when carbon black is used as the carbon source, the optimal synthesis condition of SiC-B_4C composite powders is 1550 °C for 2 h.

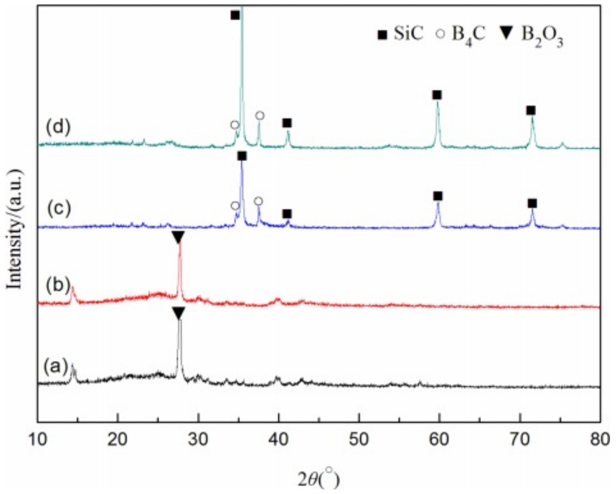

Fig. 3. XRD patterns of synthesized powder samples with carbon black as the carbon source at different temperatures: 100 °C, (b) 1350 °C+2 h, (c) 1450 °C+2 h, and (d) 1550 °C+2 h.

Fig. 4 shows the XRD patterns of the precursor mixed powder and the powder samples prepared after incubation for 2 h at different reaction temperatures with 10 wt% excess starch. Mainly B_2O_3 diffraction peaks are in the XRD pattern of the precursor mixed powder. At 1450 °C, in addition to the diffraction peaks of B_2O_3, weaker SiC diffraction peaks are seen in the synthesized powder samples. When the reaction temperature increases to 1550 °C, the diffraction peaks of B_2O_3 disappear, and only the characteristic diffraction peaks of SiC and B_4C exist in the synthesized product,

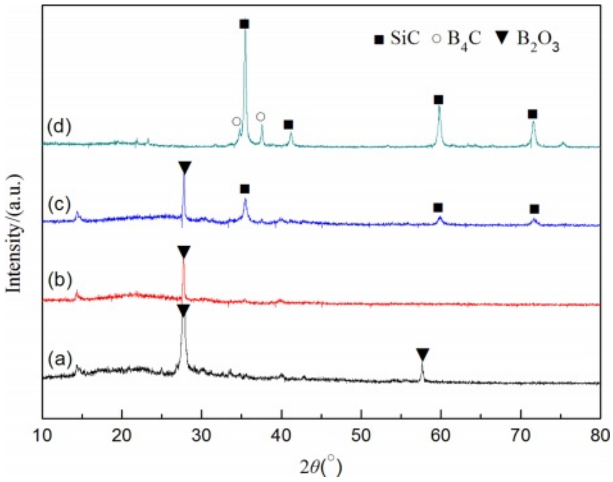

Fig. 4. XRD patterns of synthesized powder samples at different temperatures using starch as the carbon source (excess 10 wt% by mass): 100 °C, (b) 1350 °C+2 h, (c) 1450 °C+2 h, and (d) 1550 °C+2 h.

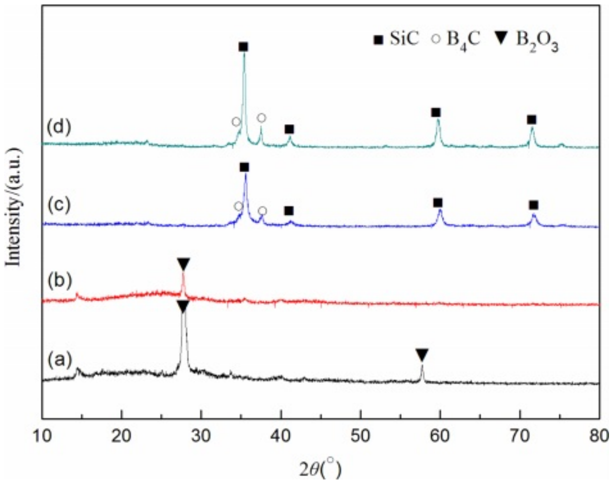

Fig. 5. XRD patterns of synthesized powder samples at different temperatures using starch as the carbon source (excess 20 wt% by mass): 100 °C, (b) 1350 °C+2 h, (c) 1450 °C+2 h, and (d) 1550 °C+2 h.

indicating that the synthesis reaction of SiC-B$_4$C composite powders is completed at the reaction temperature of 1550 °C. Based on the above analysis, when the starch is excessive by 10 wt%, the optimal reaction condition for the synthesis of SiC-B$_4$C composite powders is 1550 °C for 2 h.

Fig. 5 shows the XRD patterns of the precursor mixed powder and the powder samples prepared after incubation for 2 h at different reaction temperatures with 20 wt% excess of starch. Compared with Fig. 4, only characteristic diffraction peaks of SiC and B$_4$C exist in the powder samples synthesized at 1450 °C, indicating that a sufficient amount of starch can provide greater amount of carbon, which is beneficial to the synthesis reaction in the system. When the reaction temperature increases to 1550 °C, the XRD patterns of the synthesized powder samples do not change remarkably, but the peak shape of the diffraction peaks is sharper, indicating that the grain size of SiC and B$_4$C produced under this reaction condition is larger, and the crystallinity of the powder is better. When the starch is excessive by 20 wt%, the optimal reaction conditions for synthesizing SiC-B$_4$C composite powders are kept at 1450 °C-1550 °C for 2 h.

Microstructure and energy spectrum analysis

Fig. 6 shows the SEM images of the powder samples synthesized at 1550 °C for 2 h with carbon black as the carbon source. The powder samples are mainly composed of a large number of flaky, columnar-like particles (about 200-500 nm in diameter) and a certain number of spherical particles and irregular polyhedral particles (about 100-200 nm in diameter). The phenomenon of mutual cohesion or agglomeration between particles is less, and a diverse microstructure is formed. According to the previous XRD pattern analysis (see Fig. 3),

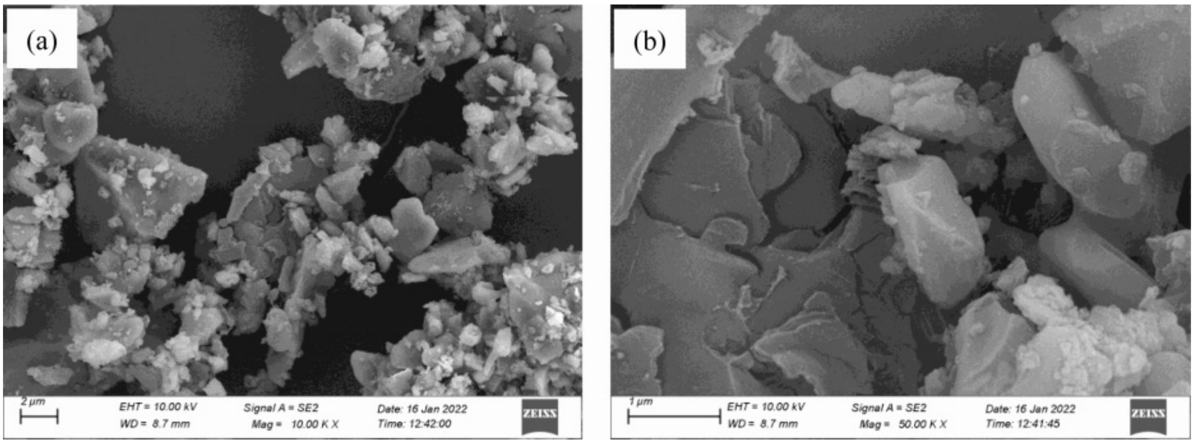

Fig. 6. SEM images of powder samples synthesized at 1550 °C for 2 h using carbon black as the carbon source: ×10000 and (b) ×50000.

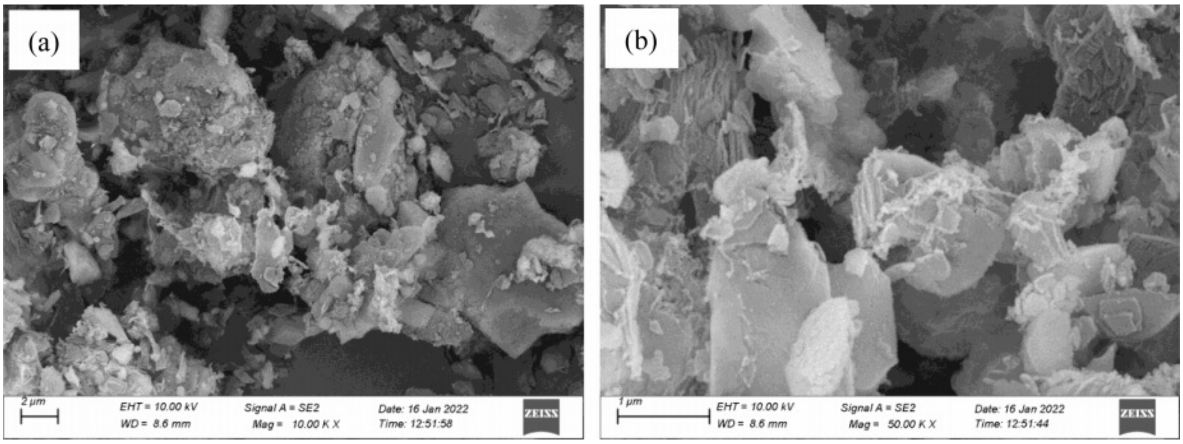

Fig. 7. SEM images of powder samples synthesized at 1550 °C for 2 h with 10 wt% excess of starch: ×10000 and (b) ×50000.

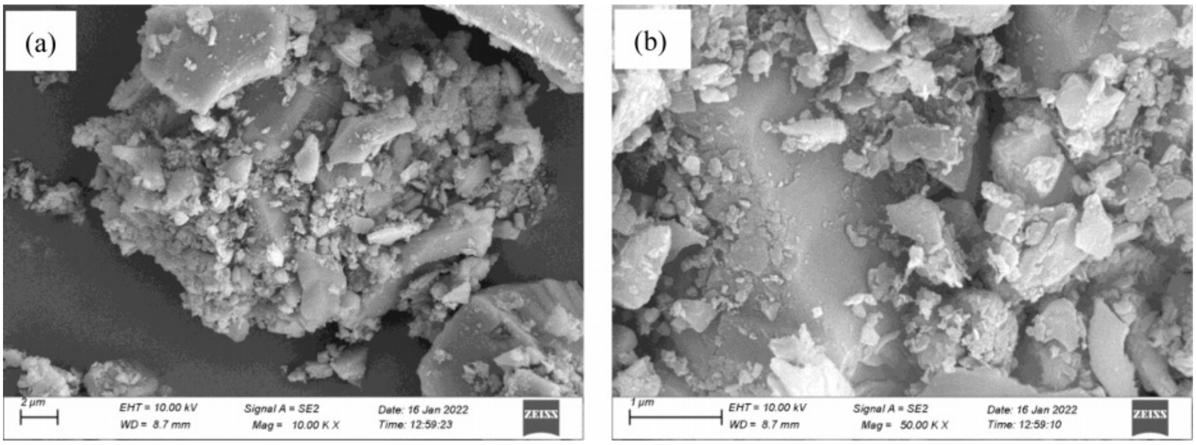

Fig. 8. SEM images of powder samples synthesized at 1550 °C for 2 h with 20 wt% excess of starch: ×10000 and (b) ×50000.

mainly diffraction peaks of SiC and B_4C are observed in the powder samples. Combined with the crystal structure and the subsequent EDS analysis, the flaky, columnar-like particles should be B_4C particles, some of the polyhedral particles may be B_4C particles generated by the LS mechanism [28], and other irregular polygonal particles should be SiC and B_4C mixed particles.

Fig. 7 shows the SEM image of the powder samples obtained by incubating at 1550 °C for 2 h with 10% excess of starch. In addition to a certain amount of flake particles, spherical particles, and other irregular structure particles (with a particle size of about 200-500 nm), a certain amount of uniform, slender whiskers are in the synthesized powder samples (the diameter is about 50-100 nm), and a certain overlap and winding phenomenon is between the whiskers. According to the crystal structure and subsequent EDS analysis, the flaky particles, spherical particles, and other irregular structure particles in the powder samples should be mixed particles of SiC and B_4C generated in the system, whereas the whisker-like substances should be SiC generated by the vapor-solid (VS) mechanism [29]. At present, the synthesis of SiC whiskers at home and abroad has two main mechanisms: the vapor-liquid-solid mechanism and the VS mechanism. The formation of SiC whiskers mainly follows the VS mechanism during the carbothermic reduction reaction without additives. In this paper, the SiO_2 in the silica sol raw material reacts with the elemental carbon generated by the decomposition of the starch raw material at high temperatures to form SiO and CO, then a part of SiO and elemental carbon form SiC particles through the VS reaction, and the other part of SiO and CO generate SiC nuclei through the vapor-vapor reaction. Under suitable conditions, the SiC nuclei seek to grow along a specific direction to generate SiC whiskers [30].

Fig. 8 shows the SEM images of powder samples synthesized at 1550 °C for 2 h with 20 wt% excess of starch. Comparing Figs. 7 and 8 reveals that the microstructure of the powder samples synthesized at 1550 °C changes with the increase of the amount of starch in the reaction system.

Fig. 9 shows the SEM images and EDS analysis results of powder samples synthesized at 1550 °C for 2

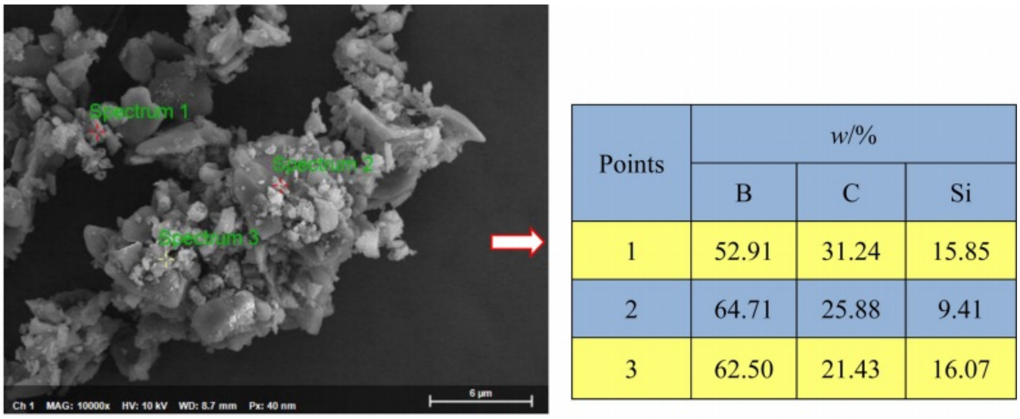

Points	w/%		
	B	C	Si
1	52.91	31.24	15.85
2	64.71	25.88	9.41
3	62.50	21.43	16.07

(a) carbon black

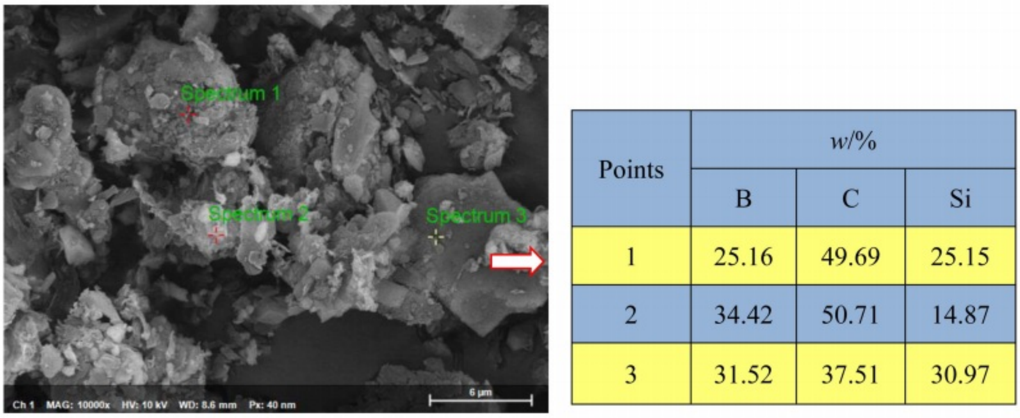

Points	w/%		
	B	C	Si
1	25.16	49.69	25.15
2	34.42	50.71	14.87
3	31.52	37.51	30.97

(b) 10 wt% excess of starch

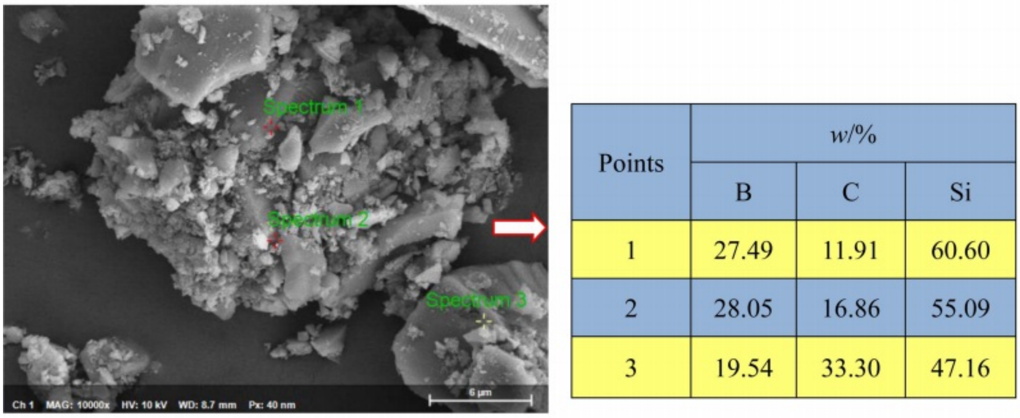

Points	w/%		
	B	C	Si
1	27.49	11.91	60.60
2	28.05	16.86	55.09
3	19.54	33.30	47.16

(c) 20 wt% excess of starch

Fig. 9. SEM images and EDS analysis results of powder samples synthesized at 1550 °C for 2 h with carbon black or starch as the carbon source.

h with carbon black or starch as the carbon source. The synthesized product mainly contains three elements, C, Si and B, indicating that the SiC-B$_4$C composite powders are successfully synthesized under this reaction condition.

Conclusions

The synthesis of SiC-B$_4$C composite powders can be promoted by increasing the calcination temperature with carbon black or starch as the carbon source. Compared with the precursor with carbon black as the carbon source, the precursor samples containing starch raw materials not only decompose to generate elemental carbon and H_2O gaseous substances during the high-temperature reaction but also generate gaseous substances such as C_xH_y, which results in a higher mass loss rate for the powder samples. The actual mass loss rate of precursor powder samples with starch as the carbon source exceeds the theoretical mass loss rate during the synthesis reaction, which is mainly caused by the escape of SiO, H_3BO_3, CO_x, C_xH_y, and other gaseous substances generated by starch decomposition in the system.

According to the analysis of mass loss rate and phase composition, the optimum condition for the synthesis of SiC-B_4C composite powders using carbon black as the carbon source or excessive 10 wt% starch as the carbon source is 1550 °C for 2 h. A sufficient amount of starch in the reaction system can provide more elemental carbon to participate in the synthesis reaction. The suitable condition for synthesizing SiC-B_4C composite powders with excess 20 wt% starch as the carbon source is 1450 °C-1550 °C for 2 h.

The powder samples synthesized with carbon black as the carbon source at 1550 °C are mainly composed of lamellar, columnar, spherical, and irregular polyhedral particles (about 100-200 nm in grain size), and the phenomenon of mutual bonding or agglomeration between particles is less. In the powder samples synthesized at 1550 °C with an excess of 10 wt% starch, in addition to a certain amount of flaky, spherical, and other irregular structure particles, a certain amount of uniform, slender whiskers (about 50-100 nm in diameter) and a certain phenomenon of lap and winding between the whiskers are observed. The whisker-like substance is SiC generated by the VS mechanism. No whisker-like substances are found in the powder samples synthesized at 1550 °C with an excess of 20 wt% starch.

Acknowledgments

This work is supported by the Key R & D Project in Hunan Province, China (Grant Number 2021GK2015) and the Planned Science and Technology Program of Hunan Province, China (Grant Number 2016TP1028).

References

1. W. Zhang, S. Yamashita, and H. Kita, J. Mater. Res. Technol. 9 (2020) 12880-12888.
2. A. Baux, S. Jacques, A. Allemand, G.L. Vignoles, P. David, T. Piquero, M.P. Stempin, and G. Chollon, J. Eur. Ceram. Soc. 41 (2021) 3274-3284.
3. M. Bugdayci and G. Baran, J. Ceram. Process. Res. 22 (2021) 510-516.
4. W. Zhang, X. Chen, S. Yamashita, M. Kubota, and H. Kita, ACS Appl. Nano Mater. 4 (2021) 3159-3166.
5. J. Hu, H. Peng, C. Hu, W. Guo, X. Tian, and Y. Peng, J. Ceram. Process. Res. 18 (2017) 79-85.
6. J.H. Yuan, Q.Y. Liu, Y. You, L.Y. Zeng, M.W. Bai, L.R Blackburn, W.M. Guo, and H.T. Lin, Ceram. Int. 47 (2021) 15843-15848.
7. D.Q. Minh, T.V. Khai, H.N. Minh, N.V.U. Nhi, and K.D.T. Kien, J. Ceram. Process. Res. 22 (2021) 246-251.
8. D.W. Tan, Z.Y. Lao, Z. Zhang, W.M. Guo, S.K. Sun, and H.T. Lin, J. Am. Ceram. Soc. 104 (2021) 2860-2867.
9. C. Sun, X. Lu, Y. Chen, L. Zuo, and Y. Li, J. Ceram. Process. Res. 22 (2021) 340-344.
10. X.J. Gao, Hasigaowa, M.Y. Sun, C.D. Liao, W.P. Huang, P. Man, W. Zhang, and Y.W. Zhou, Mater. Sci. Forum 999 (2020) 83-90.
11. R. Srinivasan, B. Suresh Babu, P. Prathap, R. Whenish, R. Soundararajan, and G. Chandramohan, J. Ceram. Process. Res. 22 (2021) 16-24.
12. W. Zhang, S. Yamashita, and H. Kita, J. Am. Ceram. Soc. 104 (2021) 2325-2336.
13. K. Kasraee, S.A. Tayebifard, H. Roghani, and M.S. Asl, Ceram. Int. 46 (2020) 12288-12295.
14. M. Bahamirian, F. Alipour, R.B. Golenji, L. Nikzad, M.H. Barounian, and M. Razavi, Ceram. Int. 47 (2021) 25221-25228.
15. Y.F. Song, H.X. Zhu, C.J. Deng, W.J. Yuan, and J. Ding, Rare Metal Mat. Eng. 47 (2018) 1082-1088.
16. K.F. Wang, K.C. Chou, and G.H. Zhang, Adv. Powder Technol. 31 (2020) 1940-1945.
17. A. Najafi, F. Golestani-Fard, H.R. Rezaie, and S. P. Saeb, Ceram. Int. 47 (2021) 6376-6387.
18. R. Tu, X. Hu, J. Li, M.J. Yang, Q.Z. Li, J. Shi, H.W. Li, H. Ohmori, T. Goto, and S. Zhang, J. Asian Ceram. Soc. 8 (2020) 327-335.
19. K. Liu, S. Gao, F. Meng, X. Wang, D. Nie, X. Du, and P. Xing, Naihuo Cailiao 53 (2019) 388-390.
20. A.S. Parlakyigit, and C. Ergun, J. Sol-Gel Sci. Techn. 92 (2019) 745-759.
21. X.C. Chong, G.Q. Xiao, D.H. Ding, and B. Bai, Mater. Rep. 33 (2019) 2524-2531.
22. S. Ding, G.W. Wen, T.Q. Lei, and Y. Zhou, J. Mater. Sci. Eng. 21 (2003) 165-169.
23. J. Hu, H. Xiao, P. Gao, Q. Li, and W. Guo, J. Ceram. Process. Res. 14 (2013) 77-81.
24. W.G. Fahrenholtz, J. Am. Ceram. Soc. 88 (2005) 3509-3512.
25. J.L. Hu, H.X. Peng, S.M. Wang, W.M. Guo, C.Y. Hu, and X.Y. Tian, Adv. Appl. Ceram. 116 (2017) 409-417.
26. X. Li, M.J. Lei, S.B. Gao, S. Yan, X.F. Wang, and P.F. Xing, Adv. Appl. Ceram. 118 (2019) 442-450.
27. J.L. Hu, C.Y. Hu, W.M. Guo, X.C. Wang, X.Y. Tian, and Y.X. Peng, J. Synth. Cryst. 46 (2017) 311-315.
28. X. Li, M.J. Lei, S.B. Gao, D. Nie, K. Liu, P.F. Xing, and S. Yan, Int. J. Appl. Ceram. Tec. 17 (2020) 1079-1087.
29. Y.Y. Peng, Z.Y. Meng, C. Zhong, J. Lu, W.C. Yu, and Y.T. Qian, Mater. Res. Bull. 36 (2001) 1659-1663.
30. P.C. Silva, and J.L. Figueiredo, Mater. Chem. Phys. 72 (2001) 326-331.